Sensors & Actuators: B. Chemical 370 (2022) 132384

Contents lists available at ScienceDirect

Sensors and Actuators: B. Chemical

journal homepage: www.elsevier.com/locate/snb

The effect of electroactive length and intrinsic conductivity on the actuation behaviour of conducting polymer-based yarn actuators for textile muscles

Sujan Dutta [a], Shayan Mehraeen [a], Nils-Krister Persson [b], Jose G. Martinez [a], Edwin W.H. Jager [a,*]

[a] Division of Sensor and Actuator Systems, Department of Physics, Chemistry and Biology (IFM), Linköping University, SE-581 83, Linköping, Sweden
[b] The Swedish School of Textiles, Polymeric E-textiles, University of Borås, 501 90 Borås, Sweden

ARTICLE INFO

Keywords:
Actuator
Yarn
Knit-de-knit
PEDOT: PSS/PPy
Strain
Force

ABSTRACT

Recently, electrically driven conducting polymer (CP) coated yarns have shown great promise to develop soft wearable applications because of their electrical and mechanical behaviour. However, designing a suitable yarn actuator for textile-based wearables with high strain is challenging. One reason for the low strain is the voltage drop along the yarn, which results in only a part of the yarn being active. To understand the voltage drop mechanism and overcome this issue intrinsically conductive yarns were used to create a highly conductive path along the full length of the yarn actuator. Ag plated knit-de-knit (Ag-KDK) structured polyamide yarns were used as the intrinsically conductive core material of the CP yarn actuators and compared with CP yarn actuators made of a non-conductive core knit-de-knit (KDK) yarn. The CP yarn actuators were fabricated by coating the core yarns with poly(3,4-ethylene dioxythiophene): poly(styrene sulfonic acid) followed by electrochemical polymerization of polypyrrole. Furthermore, to elucidate the effect of the capillarity of the electrolyte through the yarn actuator, two different approaches to electrochemical actuation were applied. All actuating performance of the materials were investigated and quantified in terms of both isotonic displacement and isometric developed forces. The resultant electroactive yarn exhibits high strain (0.64 %) in NaDBS electrolytes as compared to previous CP yarn actuator. The actuation and the electroactivity of the yarn were retained up to 100 cycles. The new highly conductive yarns will shed light on the development of next-generation textile-based exoskeleton suits, assistive devices, wearables, and haptics garments.

1. Introduction

Now a days smart and portable devices have gained a growing interest due to their vast range of potential applications such as sensors, real-time monitoring of health parameters, storage devices, and wearable actuators [1–6]. A special category are wearables based on textiles with integrated functions such as displays, sensing, actuation, energy harvesting and storage which have received widespread attention [7–9]. One of the major advantages of these types of devices is that they are soft, stretchable, and can be integrated in the clothing or even directly mounted on the human skin [10,11]. Typically, conductive materials are integrated into the textiles by combining advanced textile processing including knitting and weaving [12,13]. One special class of conductive materials are electroactive polymers (EAPs) that can provide mechanical actuation. Basically, EAPs are polymers that amongst others undergo shape and/or dimensional changes in response to an applied electrical field. Based on their working principle EAPs can be divided into two categories i.e., ionic EAPs and electronic EAPs. Ionic EAPs show electrically induced actuation due to the migration of ions or molecules (solvents) and include conducting polymers (CPs), ionic polymer–metal composites (IPMCs) and carbon nanotubes (CNTs). Electronic EAPs are actuated by applied electric fields and coulomb forces. Dielectric elastomers, liquid-crystal polymers and piezoelectric polymers belong the electronic EAP category [14–16].

Conducting polymers (CPs), such as polypyrrole (PPy), polyaniline, and poly(3,4-ethylene dioxythiophene) (PEDOT) are ionic EAPs that are

Abbreviations: CP, Conducting polymer; KDK, Knit-de-knit; PEDOT, Poly(3,4-ethylenedioxythiophene); PSS, Poly(styrene sulfonic acid); PPy, Polypyrrole; NaDBS, Sodium dodecyl benzene sulphonate; ECMD, Electro-chemo-mechanical deformation.

* Corresponding author.
E-mail address: edwin.jager@liu.se (E.W.H. Jager).

https://doi.org/10.1016/j.snb.2022.132384
Received 6 April 2022; Received in revised form 28 June 2022; Accepted 13 July 2022
Available online 16 July 2022

promising candidates as the electromechanically active materials in textile actuators due to their good mechanical properties, the large volume change, and low driving voltage [17–19]. Typically, when CPs such as PPy undergo electrochemical oxidation and reduction in contact with the surrounding ionic species, this results in swelling (and subsequent elongation) and shrinking (contraction) even at low applied potentials [20,21]. The size of the ion, as well as the types of electrolytes, also play an important role during the actuation process [22]. For a PPy actuator, when it is doped with a relatively small anion (like Cl^-), it elongates on oxidation (doping) and shortens on reduction (dedoping) and the process follows Eq. 1. On the other hand, when the PPy actuator is doped with larger anions like dodecyl benzene sulphonate (DBS^-), it elongates on reduction with cation insertion and contracts on oxidation with cation expulsion (Eq. 2) [21,23,24].

$$PPy^+(a^-) + e^- \leftrightarrow PPy^0 + a^- \quad (1)$$

$$PPy^+(A^-) + M^+ + e^- \leftrightarrow PPy^0\,(A^-M^+) \quad (2)$$

Where, a^- is small dopant anion, A^- large dopant anion, and M^+ cation from supporting electrolyte.

Keeping in mind the electrochemically induced volume change of PPy, it is possible to induce electrochemical actuation when the PPy is coated onto yarns or the surface of textiles [12]. The actuation mechanism of CP yarns is illustrated in Fig. 1. The electrochemically induced volume change is now converted in a reversible length change of the yarn actuator. The main difference between the CP yarn actuator and typical CP actuators is the structure of the actuator: Most CP actuators are constructed as a short free-standing CP film or as a bending bilayer by depositing the CP layer on a flexible (conductive) substrate. In the yarn actuator, the PPy layer is formed on the PEDOT coated yarn. This conductive PEDOT coating is required to enable electrosynthesis of PPy on the typically non-conductive yarn or textile. Therefor the actuation performance is also highly dependent on the mechanical properties of the core yarn, i.e. on the type of yarn, such as the material properties (cotton, polyamide, polyester) [25] and the structure/construction of the yarn (staple yarn, multifilament, textured) [26]. For instance, in the case of Maziz et al. PPy was coated on very stiff lyocell yarns giving a strain less than 0.1 %, much lower as seen for free-standing film PPy, illustrating that the core yarn mechanically impeded the movement. However, when coating on more stretchable elastane yarns, the strain was increased to 0.3 %[12]. Maziz et al. proposed metal-free textile-actuators using both vapour phase polymerization to provide the yarns with electrical conductivity and liquid phase electrochemical synthesis of highly actuating PPy on top and studied their performance as linear actuators [27].

Another difference between the yarn actuators and the free-standing CP film actuators or CP bilayer actuators is the voltage drop along the length of the yarn actuator. In the free-standing film case, the CP strip is often short, less than 1 cm and in a typical bilayer actuator, a uniform CP layer is formed on a flexible conductive substrate. In both cases this voltage drop is minimal. For the free-standing film because of the short length and for the bilayer due to the conductive substrate. While for the yarn actuators the actuation performance not only depends on the CP thickness and electrolyte, but also depends on the conductivity of the PEDOT coating, which depends number of coating or density of PEDOT on the yarn [24]. Basically, due to the electrical resistance of the conducting polymer the applied potential may decrease along the length, thereby reducing the actuator performance. If the conducting polymer coating is long there can be a considerable potential drop due to resistance when voltage is applied at one end [28,29]. This is often addressed as the iR drop. To overcome this iR drop different strategies have been taken. One of the most popular methods is to add a so-called current collector, e.g; by coating the CP on a highly conductive layer along the polymer strip [30]. Another solution is to use a spiral metal wire around the polymer as the current collector. Ding et al. developed a high-performance conducting polymer actuator utilising a tubular geometry and helical wire interconnects that provided up to 5 % axial strain [31,32]. Hutchison et al. designed a PPy based electrochemical actuator where the PPy was first coated onto Pt-coated polyester fibres and compared the stress generated by unplatinised with platinised PPy film and found six-fold higher force density compared to unplatinised films [33]. This increase in force generated by the platinised film was assumed to be due to better conductivity along the length of the sample. Other authors also worked to enhance the electrical conductivity of the conducting polymer itself by various methods such as physical vapour deposition, chemical vapour deposition, and electroplating methods [34–36]. In addition, the effect of extra mechanical contact length in most the actuator system has been ignored. Basically, when a polymer sample is immersed in the solution, it undergoes a free swelling phase [37], however, there is a chance for a capillary rise as well as for actuation through the extra length of the polymer, which is in air. In our work, we also try to understand the effect of the extra length present in the polymer too.

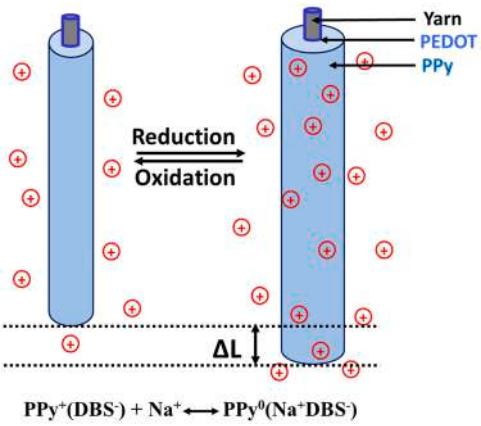

Fig. 1. A sketch of the actuation mechanism of the CP yarns. When the CP layer, doped with large immobile anions, is reduced, cations are inserted which causes an increase in the volume and thus an increase of the yarn length.

In this work, we will investigate the effect of intrinsic conductivity of the yarn actuator in more detail and address the effect of the so-called iR drop on the actuation of yarn actuators by varying the active length of the yarn actuators. For this we chose two knit-de-knit (KDK) structured polyamide yarns: a non-conductive and an intrinsically conductive (Ag plated) yarn. Silver was selected due to its high electrical conductivity. To further elucidate the mechanism and the effect of the passive contact length, and the possibility of capillary transport of the electrolyte, we applied two different approaches to vary the active length of the electrochemical actuation of the yarn in the electrolyte solution. In the first approach, after applied preload, the actuation behaviour of active yarns length was measured by changing the ratio of the yarn submerged in the electrolyte, i.e. by increasing the level of the electrolyte in the electrochemical cell. In the second approach, we changed the actual length of active yarn, i.e., by cutting the yarn, and actuation behaviour was again measured under an applied constant pre-load. Due to the limited conductivity along the yarn, a voltage drop may occur, along the length of the film during the linear actuation, which influences the performance [33]. The actuation properties of PPy doped polyamide yarn and inherent silver-plated conductive yarn were investigated in terms of isotonic displacement and isometric force.

2. Experimental section

2.1. Materials

Knit-de-knit (KDK) structured polyamide yarn (dtex=110, no of filaments=51) was purchased from Chapman Fraser Co, England and silver-plated knit-de-knit (Ag-KDK) polyamide yarn (dtex=110, no of

filaments=34, no of twist per meter=2) was purchased from Statex Produktions & Vertriebs GmbH, Germany, and both yarns used as received. Pyrrole was purchased from Sigma and distilled under vacuum before use and stored at − 20 °C. Polyethylene glycol (PEG400) was purchased from Kebo AB and used as received. Dimethyl sulfoxide (DMSO), sodium dodecyl benzene sulphonate (NaDBS) were also purchased from Sigma Aldrich and used as received. PEDOT:PSS PH 1000 was obtained from Heraeus Company. Ultrapure water (18.2 MΩ) from Millipore Milli-Q equipment was used in all experiments.

2.2. Coating of conductive yarn

Adapting the concept that PEG and DMSO enhance the conductivity and linear actuation behaviour [38], here we used 20vol % of DMSO and 10 wt % of PEG400 in PEDOT:PSS solution to make PEDOT:PSS/PEO/DMSO. In this work, we address PEDOT:PSS/PEO/DMSO as PEDOT in all cases unless otherwise stated. The fabrication is schematically summarised in Fig. 2a. Conductive yarns were prepared by a simple two-step method. First, 300 mm long pieces of bare yarns were passed at a speed of approximately 10 mm/s through a 150 mm long U-shape tubing containing the PEDOT polymer solution and thereafter left to dry for 2 h. The coating was repeated for 4–5 times for KDK yarns and 15–16 times for Ag-KDK yarn to ensure sufficient conductivity and weight per unit length around 2×10^{-5} g/mm in every case. It is to be noted that we tried to synthesise PPy directly on the Ag-KDK yarn by electrochemical polymerisation, but polymerisation did not happen uniformly on the yarn. This is possibly due to the fact that the PPy polymerized predominantly on the conducting Ag particles in the yarns [17] and the increased passivation of the Ag particles due to possible oxidation of the Ag at potentials lower or similar to what is required for the electropolymerization [39]. To achieve a uniform PPy polymerisation, we first coated Ag-KDK with PEDOT. This layer was deposited on the yarn as a "seed layer" to form a stable uniform conductive surface, followed by the deposition of the actuating PPy layer. The weight per unit length of the coated yarns was measured gravimetrically and calculated at room temperature with the following equation:

$$\text{Weight per unit length (g/mm)} = (W_f - W_i)/300$$

where W_f is the weight of the coated yarn after drying and W_i is the weight of the initial uncoated yarn and 300 is the length of the yarn in mm to obtain the PEDOT mass deposited by length.

The resistance of the yarns was measured using a Multimetrix DMM220 digital multimeter over 60 ± 0.01 mm yarn length by connecting hook clip test probes at the two ends.

2.3. Electro-polymerisation

All the electro-chemo-mechanical deformation (ECMD) experiments were performed in a single-compartment three-electrode electrochemical cell with a diameter of 4 cm. For electro-polymerization and cyclic voltammetry, the three-electrode cell was connected to an Ivium CompactStat.h potentiostat (Ivium Technologies, The Netherlands) and the included Ivium software was used. Stainless steel fabric was used as a counter electrode (CE), which was placed around the cell wall. The working electrode (WE), i.e. the yarn, was set in the centre of the cell and a BASi MF-2052 Ag/AgCl (3 M NaCl) reference electrode (RE) was set near the upper part of WE. All potentials referred in this work are related to this RE. An 80 mm long PEDOT coated yarn was mounted using a plastic screw (0.522 g) at the lower end as weight and the upper part of the yarn was connected to the WE are using a nickel-plated steel alligator clip (Mueller Electronic, bought from Elfa Distrelec). It is to be noted that exactly 60 mm of the PEDOT coated yarns was immersed in the electro-polymerization solution. The polymerization was performed in 0.1 M NaDBS and 0.1 M pyrrole aqueous solution by applying a constant current of 0.5 mA through the yarns for 20,000 s at room temperature. After the synthesis, the yarns were washed thoroughly with DI water to remove excess pyrrole and NaDBS. The yarns were left in air to dry and stored for further measurement at room conditions (22 °C). It should be noted that after polymerization with PPy the yarns will be addressed as PPy/KDK or PPy/Ag-KDK yarns. Cyclic voltammograms of yarns were performed between − 1.2 V and 0.2 V at 10 mV/s scan rate in 0.1 M NaDBS aqueous electrolyte at room temperature.

2.4. Electrochemomechanical deformation (ECMD) measurement

All ECMD were performed in a single-compartment three-electrode electrochemical cell in a liquid electrolyte and the experimental setup is shown in Fig. 2b. For this measurement, a CP coated yarn of chosen length was firmly clamped with a hook grip clip at one end and test lead with 4 mm laboratory plug at the other (Pomona Electronic, bought from Elfa Distrelec) and glued at the lower end. The upper part is fixed to a lever arm transducer. The lever arm, though its associated servo controller (Cambridge Technology Inc. Model 200B, USA), is connected to a computer using the potentiostat analogue-in port and the signal is

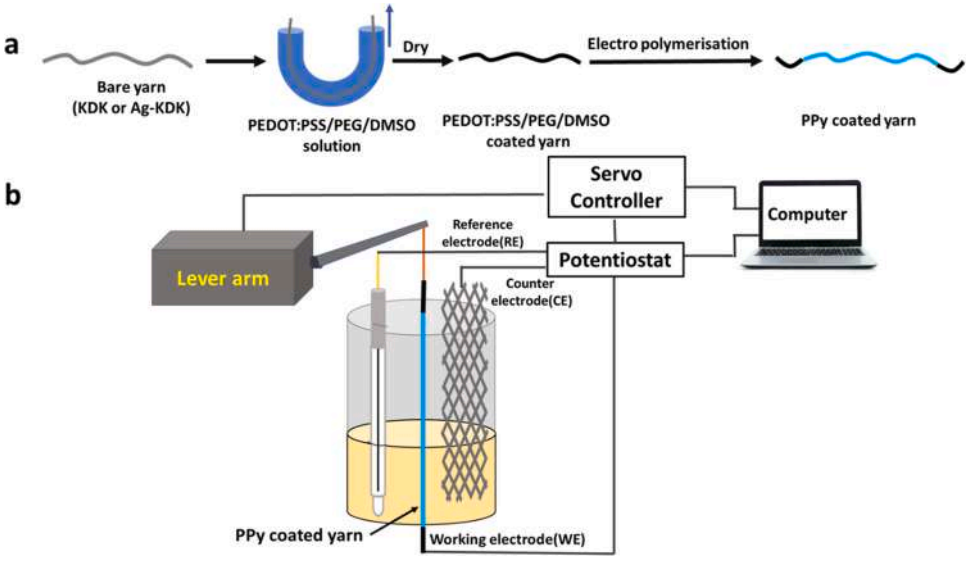

Fig. 2. Schematic diagram of (a) coating of PEDOT and PPy on the KDK or Ag-KDK yarn to fabricate the yarn actuators and b) the experimental setup to measure the isotonic strain or isometric force.

recorded using the Nova 2.1 software of the Autolab PGSTAT204 (Metrohm Autolab) used to apply the electrical stimuli. The lever arm settings were controlled through the nobs on the frontal panel of the lever arm servo controller. The lever arm was used to measure displacement and force under isotonic or isometric conditions, respectively. A stainless-steel mesh was used as CE and inserted in the cell, and a BASi MF-2052 Ag/AgCl (3 M NaCl) RE was set in the upper part of the 0.1 M NaDBS electrolyte. All yarns were immersed in the electrolyte for 30 min before the measurement. For each system, three samples were prepared and measured independently.

The ECMD actuation of the yarn actuators was performed by following two different approaches (Fig. 3). In the first approach (Method A, Fig. 3a), an 80 mm long yarn actuator was mounted into the lever-arm and an initial preload (12.5 mN) was applied to the yarn. This 80 mm yarn length can be subdivided into four parts. From top to bottom: a 10 mm mechanical contact portion to ensure a mechanical connection with the lever arm, a portion outside the electrolyte, a wet portion immersed in the electrolyte solution, and a 10 mm lower portion allowing the connection as a WE. For example (Fig. 3a), a 20 mm active yarn length means out of the 80 mm yarn length, the initial 10 mm was mechanical contact portion, next 40 mm was in the air, then 20 mm length of yarn was immersed into the 0.1 M NaDBS electrolyte solution, and the lower 10 mm connected through the hook clip to the WE. For the actuation study, step potentials (−1.2 V and +0.2 V) were applied to the electrochemical cell for 600 s. In the same way, the strain (%) measurement of 30, 40, 50, and 60 mm immersed yarns were done by adding the requisite amount of electrolyte solution in the cell. Force measurements were also done using the same set-up but by changing the measurement mode of the servo controller from isotonic to isometric.

In the second approach (method B, Fig. 3b), at first an 80 mm yarn actuator was mounted in the lever arm machine as described previously. It is to be noted that here actuation was started from 60 mm yarn immersed. The actuation study of 60 mm yarn is the same as method A. After the actuation study, isometric force measurements for 60 mm immersed length were also done by changing the setting. After completion of the measurements, the yarn was washed thoroughly with ultrapure water to remove excess surface ions and dried at room temperature. For the next experiment, the yarn was cut to 70 mm. Now, the total immersed length of the yarn was 50 mm, which means 50 mm yarn immersed inside the electrolyte solution and the remaining 20 mm yarn connected at both ends (10 mm at the top for mechanical connection and 10 mm at the bottom for electrical connection). Then, the same actuation and force measurements were taken. Next, the yarn was cut to 60 mm to get 40 mm immersed length actuation measurement, and so on. It is also to be noted that for different immersed length yarns, different sizes of electrochemical cells were used. To study 60 mm immersed yarn length, a 70 mm length cell was used, again for a 50 mm immersed yarn length, a 60 mm length cell was used, and so on.

The strain (%) was calculated from the formula $Strain\ (\%) = \frac{\Delta L}{L} \times 100$, where ΔL= displacement of the PPy coated yarn and L is the starting length of the submersed part. Step potentials (−1.2 V and +0.2 V) were applied with a period of 600 s to the yarn. For the calculation, the last 5 cycles out of 10 were used and the average value was taken to determine strain (%) using the above equation. All the measurements were done three times, and the average value was taken.

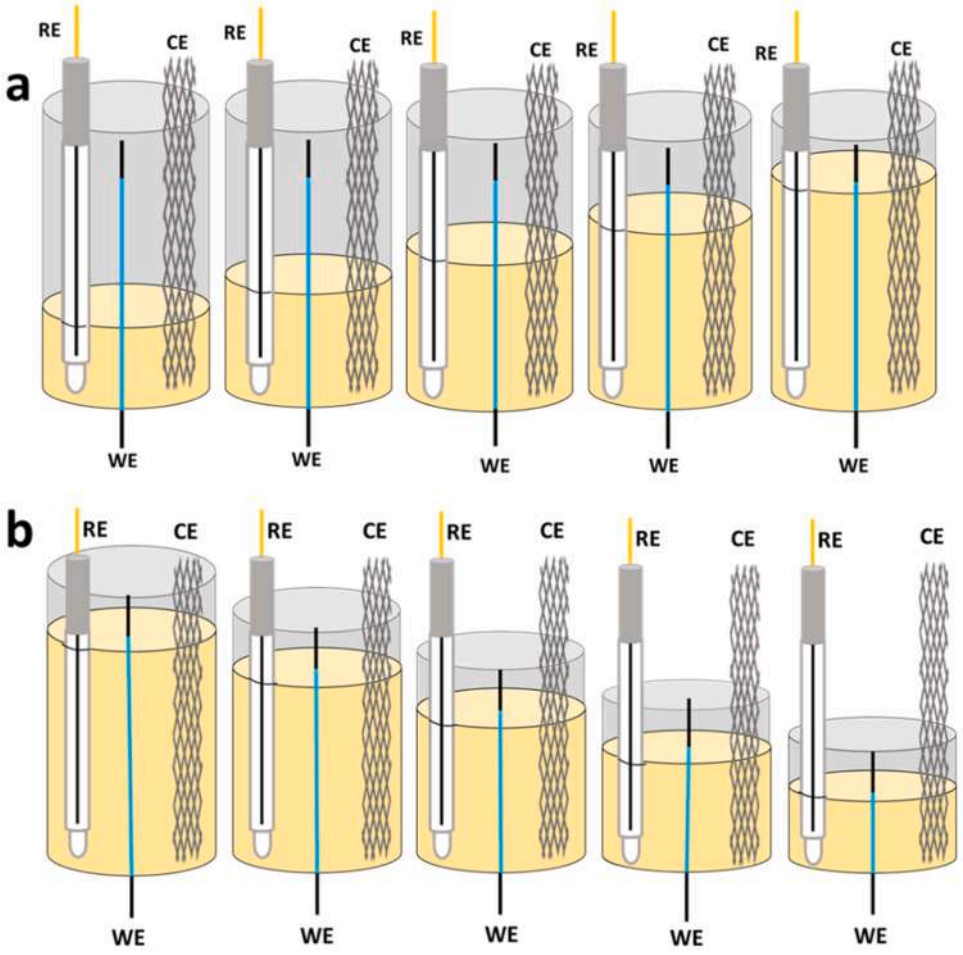

Fig. 3. Schematic diagram of two different approaches for electro-chemo-mechanical actuation of the yarn actuators (a) for method A, varying the electrolyte level and (b) for method B, varying the yarn length.

3. Results and discussion

3.1. Electro polymerization of yarn

The schematic diagram of the synthesis of yarn actuators is shown in Fig. 2. First, the commercial bare yarns (KDK- polyamide or Ag-plated KDK polyamide) were coated with the PEDOT solution and a successful diffusion of the PEDOT solution into and subsequent coating onto the yarns was evidenced by the formation of deep blue-colored yarns (Figs. 4a and 4b). The resistance of PEDOT/KDK and PEDOT/Ag-KDK increased linearly with the yarn length following the standard Ohm's law, resulting in an iR drop along the yarn length, and the max resistances were 700 Ω, and 20 Ω, respectively, for 60 mm yarn length (Fig. 4c). Having ensured that the conductivity was sufficient, the dried PEDOT coated dark, blue-colored yarns were electropolymerized in 0.1 M NaDBS/PPy solution. The electro-polymerization chrono- potentiograms of PPy/KDK and PPy/Ag-KDK are shown in Fig. 4d and the curves showed almost the same behaviour.

In the beginning, potential increased, then decreased, and finally reached a steady potential, which indicates the uniform deposition of PPy on PEDOT coated yarns (Fig. 4d) [40]. The potentials developed for KDK yarns were higher, in the range ~0.71 V, than for Ag-KDK which was ~0.62 V. This can be explained as PEDOT/Ag-KDK yarns were more conductive in comparison to PEDOT/KDK yarns, which lowered the potential. Visual inspection further confirmed a good PPy coating on the PEDOT/KDK or PEDOT/Ag-KDK yarns as the yarns turned from dark

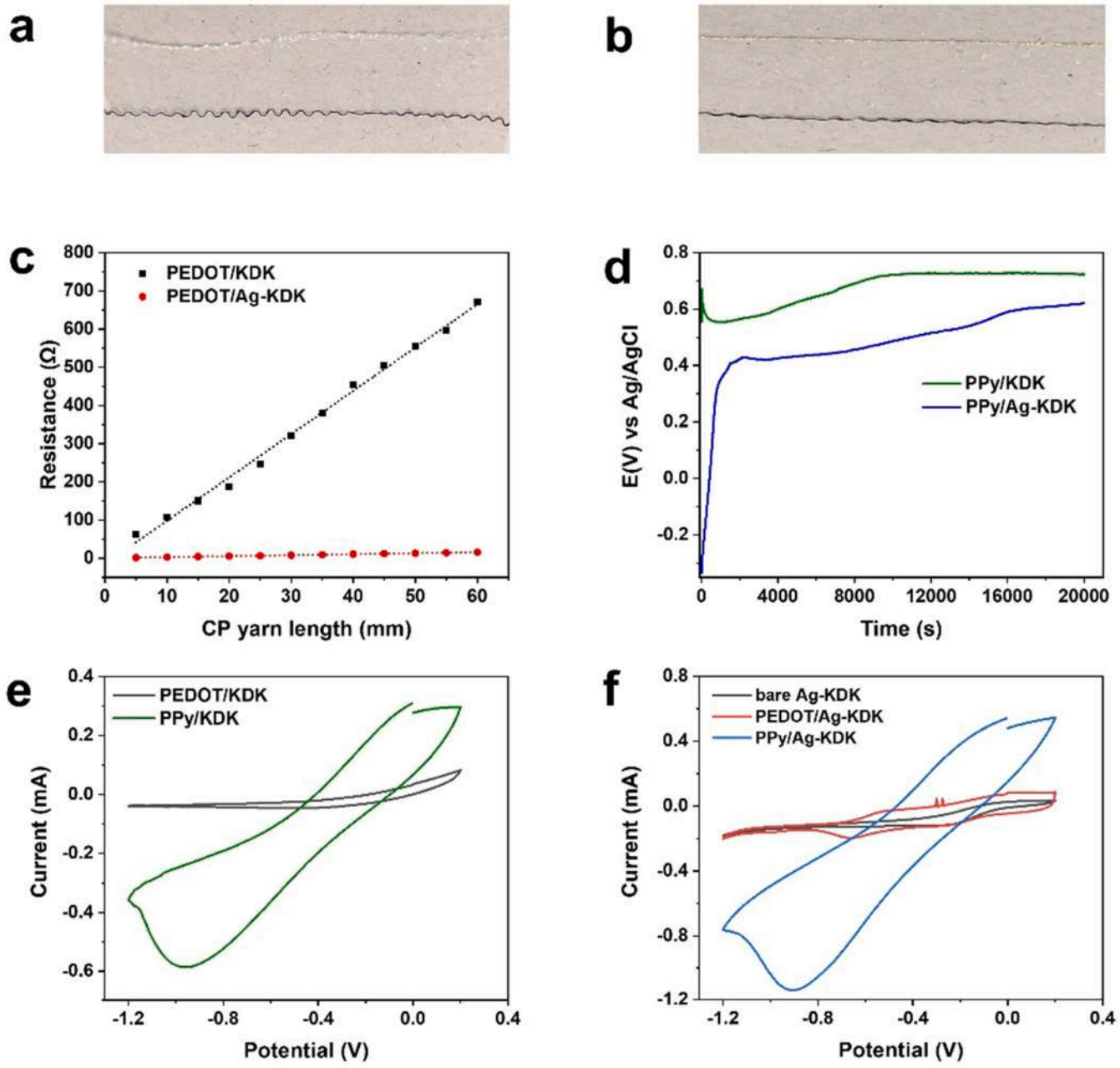

Fig. 4. Photographs of (a) bare and PEDOT coated KDK yarns and (b) bare and PEDOT coated Ag-KDK plated yarns. (c) Effect of CP yarn length on the resistance (d) Electro polymerisation of PPy/KDK and PPy/Ag-KDK yarns in a three-electrode cell (galvanostatic, 0.1 mA/cm2,20,000 s) in (0.1 M PPy+ 0.1 M NaDBS) solution. Cyclic voltammograms of (e) PEDOT/KDK and PPy/KDK yarn (f) bare Ag yarn, PEDOT/Ag-KDK and PPy/Ag-KDK yarn in 0.1NaDBS solution between − 1.2 V and + 0.2 V versus Ag/AgCl at scan rate 10 mV/s at room temperature.

blue to black.

Cyclic voltammetry also was carried out to investigate the electroactivity of the PEDOT and PPy coated yarns in 0.1MNaDBS aqueous solution between − 1.2 V and + 0.2 V versus Ag/AgCl at room temperature. Figs. 4e and f show the corresponding cyclic voltammograms for KDK and Ag-KDK yarns respectively. In Fig. 4f we also included the CV of the bare Ag-KDK yarns to compare all Ag-KDK yarn variants, since the bare Ag-KDK yarns are also conductive and may possess some electroactive response. After electro polymerisation of PPy, a higher current can be observed in the case of PPy/KDK as compared to PEDOT/KDK (Fig. 4e) as well as for PPy/Ag-KDK as compared to PEDOT/Ag-KDK, indicating a good PPy coating. In addition, the usual PPy redox peaks are clearly visible. In both cases, it is possible to observe a ~5-fold increment of the current passing through the electrode after PPy coating, indicating a good PPy deposition and that the main source of electroactivity of the actuator yarns will be the PPy coating.

3.2. Linear actuation measurement

PPy/KDK and PPy/Ag-KDK yarns were investigated for their linear actuation using ECMD under isotonic conditions driven by square potential waves. Fig. 5 shows the movement (contraction/expansion) during oxidation/reduction of a 50 mm immersed yarn as a response to the cycling of the potential between − 1.2 V and + 0.2 V at a constant load of 12.5mN under a square wave function having a 600 s period for 10 cycles. This movement confirms that the motion is driven by the exchange of cations (Na^+), according to electrochemical reaction 2 (Eq. 2). The upward part of the curve represents the expansion during reduction and the downward curve the contraction during oxidation. In most of the cases, we used the reduction values unless otherwise stated. The length of immersed portion was 50 mm. The curve shows reversible oxidation contraction, reversible reduction expansion and irreversible stain (%). Green line is an envelope curve showing approximately baseline.

Further, it can be seen that the first reduction is higher in irreversible strain, which is commonly seen in PPy actuators [41]. The actuation of PPy/DBS yarns showed both reversible as well as irreversible expansion. The initial cycles showed both irreversible and reversible expansion and once the irreversible expansion has reached a maximum value, the actuation stabilizes and showed reversible expansion only [42]. This is called the steady-state of the yarn actuator. From Fig. S1a, we can see that the steady-state was reached after 100 cycles and the reversible strain remained almost constant. Fig S1b shows the charge (C) vs time plot and we can see that the consumed charge, that correlates to the reversible strain, was stable too. In Fig. 5 it can be seen that the irreversible strain after 10 cycles was 0.38 % and the reversible strain was 0.19 % for the yarn actuator immersed in 50 mm electrolyte (method A).

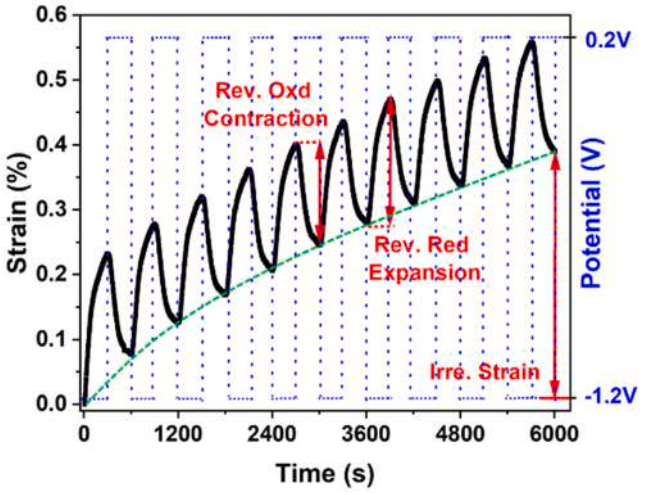

Fig. 5. Isotonic strain (%) under a square wave potential step for PPy/KDK yarn with time(s) for 10 cycles in 0.1 M NaDBS solution in the potential range − 1.2 V to + 0.2 V under 12.5mN load.

The effect of immersed yarn length on the strain and displacement measurement is shown in Fig. 6. As we know the actuator performance depends on the length, size, and as well as geometry. So, in our study, we try to find the effect of active length during actuation. The active length should corelate to the length immersed in the electrolyte solution and depend on the iR drop (Fig. 4c). For method A, the experiments started from 20 mm to 30, 40, 50, and 60 mm to measure the yarn actuator elongation and contraction. The maximum reversible electrochemical strain for PPy/KDK yarn was 0.53 % for 20 mm active length. The electro-chemo-mechanical strain decreased with increasing the electrolyte level and the values for 30, 40, 50 and, 60 mm active yarn were 0.34 %, 0.24 %, 0.19 %, and 0.15 %, respectively. (Table 1). However, the absolute displacement only slightly decreased for longer lengths and became constant when more than 30 mm were immersed in the electrolyte. This can be explained as the strain value calculated as ΔL/L* 100 %, where ΔL= displacement of the PPy coated yarn and L= total active length. Since the value of the displacement was almost the same throughout the active yarn length, (L) the reduction of the strain value was an artifact due to the calculation.

Next, we performed the strain (%) and displacement actuation for PPy/Ag-KDK yarns and the trend was found to be similar to Ppy/KDK yarns (Fig. 7). With increasing electrolyte level, the strain (%) value is decreasing, whereas displacement was almost constant. The maximum strain of PPy/Ag-KDK for 20, 30, 40, 50 and 60 mm immersed in the electrolyte were 0.64 %, 0.41 %, 0.29 %, 0.23 %, and 0.20 % respectively. Fig. 8a shows the electro-chemo-mechanical strain comparison between PPy/KDK and PPy/Ag-KDK yarn. As can be seen, the PPy/Ag-KDK yarn shows more strain in comparison to PPy/KDK yarn. A 20 mm immersed yarn showed 0.53 and 0.63 strain (%) for PPy/KDK and PPy/Ag-KDK, respectively. level of PPy/Ag-KDK yarn (Method A).

Moreover, PPy/Ag-KDK yarn shows more displacement in comparison to PPy/KDK yarn (Fig. 8b). The elongation for a 20 mm immersion of PPy/KDK yarn is 0.10 mm and PPy/Ag-KDK is 0.12 mm, thus showing a 19 % increase which, we attribute to the reduction of iR drop. The reason for this is that PPy/Ag-KDK yarn is more conductive as compared to PPy/KDK due to Ag coating on the core yarn (Fig. 4c), thus the iR drop is reduced along yarn actuator which promotes more oxidation/reduction and thus more contraction/elongation. Thus, we can conclude that the conductivity of the yarn plays indeed a major role during the strain of the yarn and PPy/Ag-KDK was found more effective in comparison to PPy/KDK.

3.3. Force measurement

Fig. 9 shows the force generation during redox cycling of a 50 mm electrolyte level versus time with the potential difference between electrodes varied from − 1.2 V and + 0.2 V. It is to be noted that the graph showed a negative slope drift. The reason for this is that at the beginning of the isometric force measurement, pre-stretching causes a stress relaxation transient and showed a negative slope drift. However, in the case of strain (%), pre-stretching implies a creep transient and showed a positive slope drift [37].

The comparison of isometric force between PPy/KDK and PPy/Ag-KDK yarn by using method A is shown in Fig. 10. Thus, for PPy/KDK showed a decrease in force with increasing active yarn length, similar to the behaviour of the displacement. The force of PPy/KDK for 20, 30, 40, 50, and 60 mm were 4.77, 4.28, 3.89, 3.68 and 3.22 mN respectively. On the other hand, for PPy/Ag-KDK yarn the force showed a slight increase followed by a slight decrease with increasing the active yarn length. Moreover, it can be seen that PPy/Ag-KDK yarns generated more force as compared to the PPy/KDK yarns. For instance, the force for a 20 mm active of PPy/KDK is 4.63 mN and PPy/Ag-KDK is 5.93 mN, thus

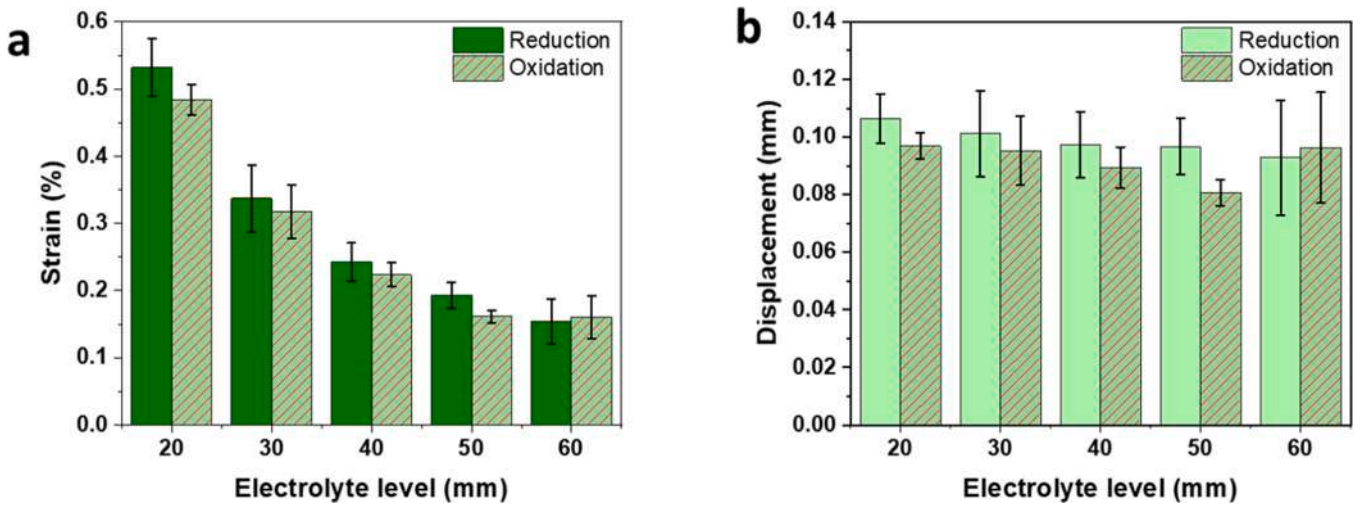

Fig. 6. (a) Strain (%) and (b) displacement measurement as a function electrolyte level. (Method A).

Table 1
Strain (%) and displacement values (reduction) of PPy/KDK and PPy/Ag-KDK yarn (Method A.

Electrolyte level (mm)	20	30	40	50	60
	PPy/KDK Yarn				
Strain (%)	0.53	0.34	0.24	0.19	0.15
Displacement(mm)	0.11	0.10	0.10	0.10	0.09
	PPy/Ag-KDK Yarn				
Strain (%)	0.64	0.41	0.29	0.23	0.20
Displacement(mm)	0.13	0.12	0.12	0.12	0.12

showing a 14 % increase for PPy/Ag-KDK yarn. We attribute this difference to the reduced iR drop (Fig. 4c), resulting in more active material thus more force generation.

3.4. Linear actuation measurement: effect of measurement method

Having shown that the PPy/Ag-KDK yarns showed more strain and displacement in comparison to PPy/KDK yarns due to the reduced iR drop, we investigated the effect of the passive part of the yarn on actuation. As mentioned earlier, in method A, a portion of the yarn was immersed in the electrolyte and the other portion was in air. For instance, when we consider a 20 mm active yarn length that means 20 mm yarn was immersed in the electrolyte whereas the remaining 40 was in air. However, in the new approach during the electro-chemo-mechanical actuation which we designate as method B, a small and constant portion of the yarn is in air, thus here the yarn showed actuation on the portion immersed in the electrolytes. It is to be noted that in all cases the mechanical contact length has been kept the same which is around 10 mm. The schematic diagram for both approaches is shown in Fig. 3.

In Fig. 11, the effect of electrolyte level on the strain and displacement measurement using method B is shown. Similar observations for strain (%) were found in method B as for method A. With increasing electrolyte level, the strain (%) was decreased. However, with an increase of electrolyte level, there is a slight increase in displacement for both PPy/KDK and PPy/Ag-KDK yarn (Fig. 11b, Table 2). Again PPy/Ag-KDK showed more strain (%) and displacement than PPy/KDK in method B too.

Fig. 12 shows a comparison between method A and B for strain (%) of PPy/KDK and PPy/Ag-KDK yarns. As can be seen, method A showed more strain (%) and displacement in comparison to method B for both PPy/KDK yarn PPy/Ag-KDK yarns. The difference was significant for 20 mm and 30 mm immersed length. With the increase of electrolyte levels, the difference in values between method A and method B was decreased and became non-significant for 40–60 mm.

The active length is determined by both the iR drop (Fig. 4c) and the

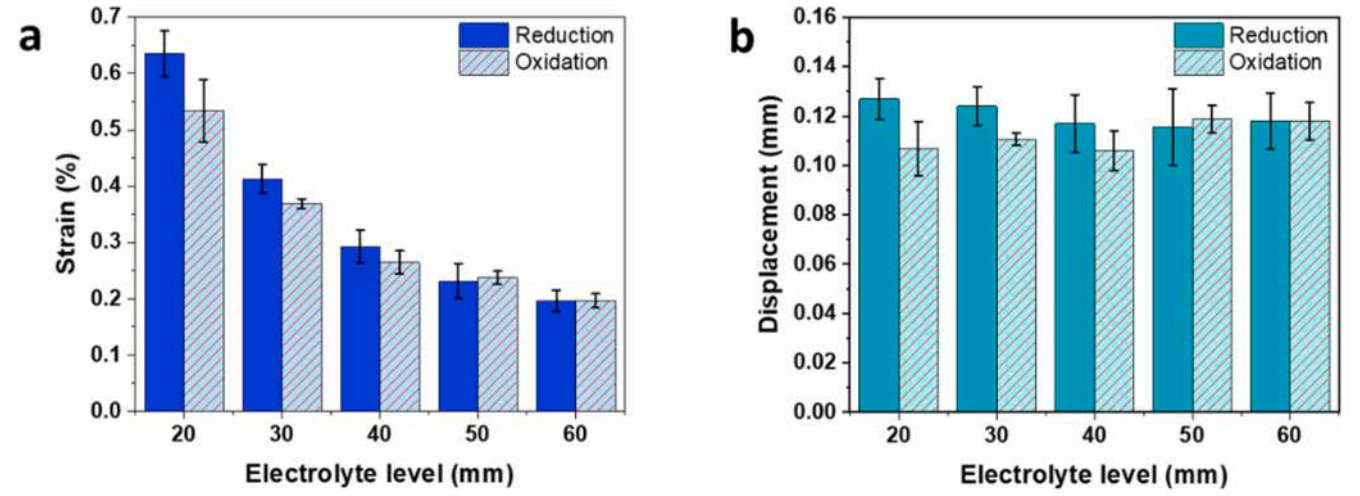

Fig. 7. (a) Strain (%) and (b) displacement measurement as a function of electrolyte level.

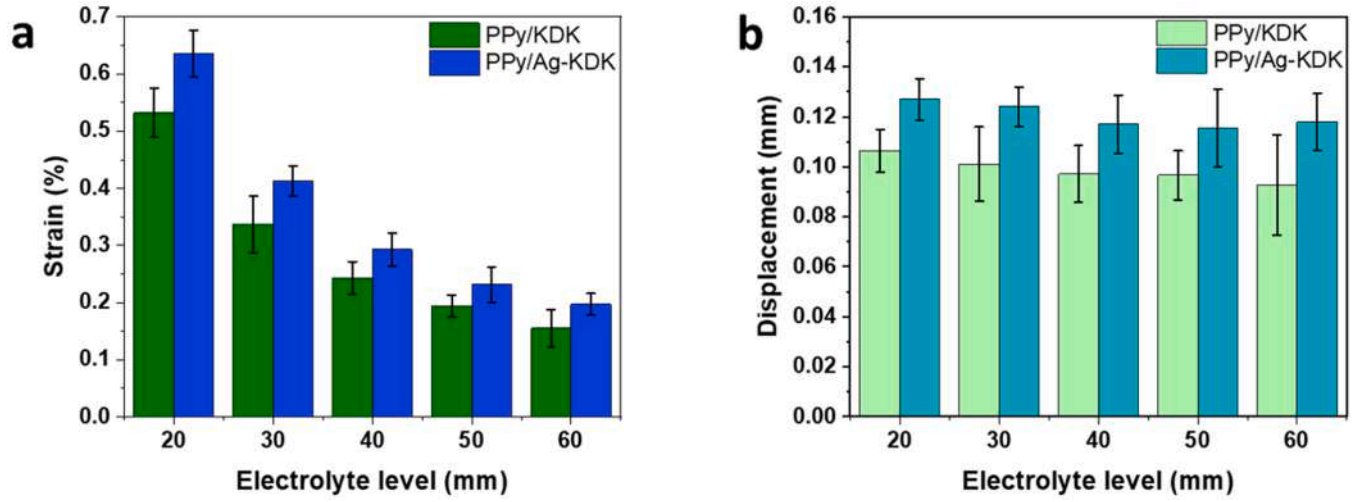

Fig. 8. (a) Strain (%) and (b) displacement comparison of PPy/KDK (and PPy/Ag-KDK yarn by using method A (reorganised from Figs. 6 and 7).

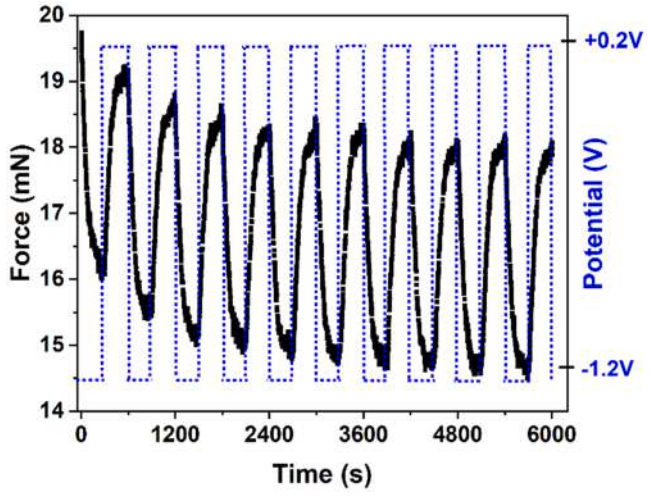

Fig. 9. Isometric force (mN) of the actuator versus time (s) for 10 cycles in 0.1 M NaDBS solution under 150mN load. The submerged length (electrolyte level) of PPy/KDK yarn is 50 mm. (Method A).

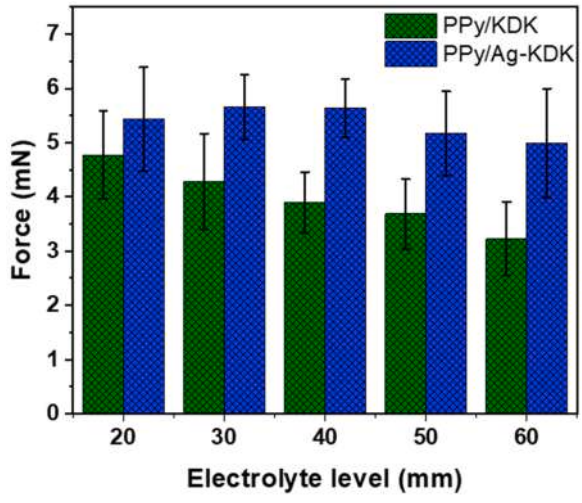

Fig. 10. Force as a function of the electrolyte level for PPy/KDK and PPy/Ag-KDK yarns using method A.

electrolyte level. Comparing the results, we can conclude that the active length is limited by the iR drop in method A, while for method B the active length is limited by the electrolyte level for the shorter lengths, but for longer lengths (40–50 mm in the case of Ag-KDK), here too the iR drop determined the active length. The discrepancy between the two methods can be explained by taking into account the capillary forces. In method A, electrolyte can go upward and thus there is a chance for capillary rise throughout the yarn. Thus, actuation can also happen in the portion of the yarn which was outside the electrolyte solution, since the potential is applied along the full yarn length and there is an access to solvent and ions in this wetted portion of the yarn. Taking into account the voltage drops along the yarn, it could still experience a low actuation in the yarn. Based on the increase in expansion up to 40 mm long yarns (Fig. 11) and strain (%) differences between method A and B up to 40 mm (Fig. 12) we estimate the wetted part above the electrolyte level to be between 20 and 10 mm. That is in the case of method A an additional 10–20 mm part of the yarn is electromechanically active thus explaining the discrepancy of the results between the two measurement methods.

To confirm the capillary flow, we prepared a colored 0.1 M NaDBS solution by using red food color dye and hang an 80 mm long bare KDK yarn in the colored solution so that 60 mm of the yarn length was present in the solution. After absorbing the solution, some colored solution was observed to rise to approximate 15 mm for both the KDK and Ag-KDK yarns due to capillary flow whereafter it reached equilibrium state, thus confirming this effect. However, in method B there is less and constant capillary rise, limiting the length which can be subjected to capillary rise every time. The schematic diagram showing the electrolyte levels of the six yarns and effect of voltage drop on the actuation for method A and method B is shown in Fig. 13. Moreover, for 60 mm yarn length, it showed similar strain (%) and displacement behaviour. For 60 mm immersed yarns the approaches are same and that is why its shows similar tendency.

To check whether this difference in the strain (%) is not an effect of the number of cycles, since the methods measure the samples in the reverse order, we measured the expansion for 100 cycles (Fig. S1). It showed that the actuation was stable and that the number of cycles (i.e. the order of testing the different lengths) could not explain the observed difference between the two methods. The electrolyte level is indicated by a solid red line, the wetted portion by the dashed red line and the iR drop, and thus the electroactivity of the PPy, by the blue colored gradient. Fig 13a1 and b1 compare the situation for a 20 mm immersed length as an example.

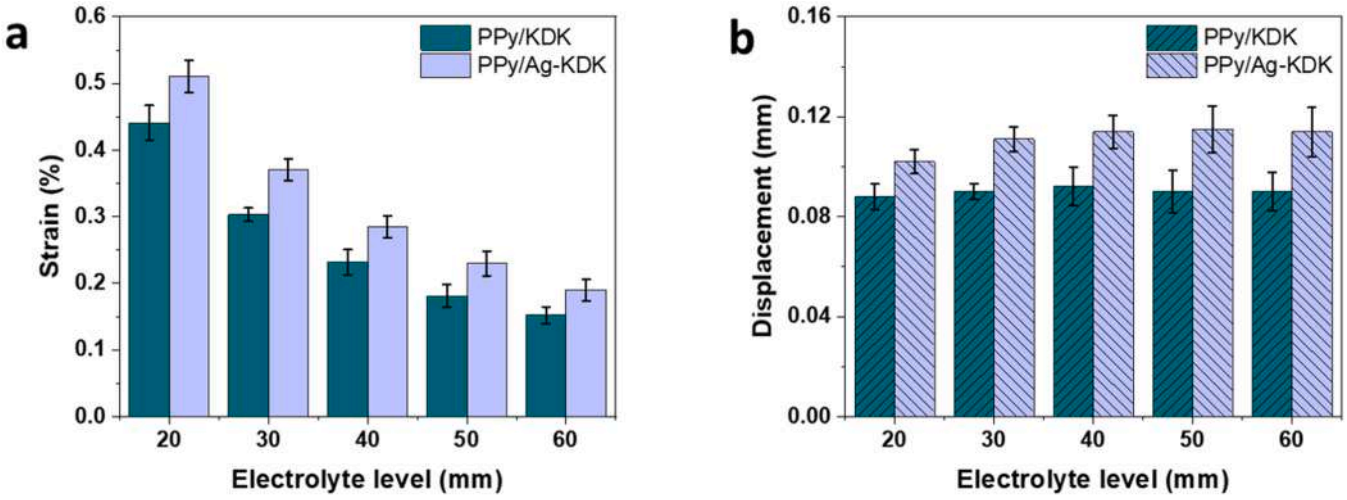

Fig. 11. Strain and displacement comparison of PPy/KDK (a) and PPy/Ag-KDK (b) yarns using method B.

Table 2
Strain (%) and displacement values(reduction) of PPy/KDK and PPy/Ag-KDK yarn (Method B).

Electrolyte level (mm)	20	30	40	50	60
	PPy/KDK Yarn				
Strain (%)	0.44	0.30	0.23	0.18	0.15
Displacement(mm)	0.09	0.09	0.09	0.09	0.09
	PPy/Ag-KDK Yarn				
Strain (%)	0.51	0.37	0.29	0.23	0.19
Displacement(mm)	0.10	0.11	0.11	0.12	0.11

4. Conclusion

Here, we studied the effect of the conductivity of the current collector, i.e.; electrical properties of the conductive yarns that form the core of the yarn actuators. The relatively low conductivity of CPs can cause a significant voltage drop along the length of the yarn actuator and thus reduce the performance. To reduce this problem, in this present work, we employed an intrinsically conductive yarn, Ag-KDK, as the core of the yarn actuator. This core yarn was turned into a soft, yarn actuator by first dip coating it with PEDOT followed by galvanostatic electro-polymerization of the PPy. It showed that using the intrinsically conductive Ag-KDK yarn as the core, the strain increased by ~19 % and force by ~4 % as compared to the non-conductive KDK core yarn. Additionally, electro-chemo-mechanical actuation was investigated using two different methods. In the first method, the actuation behaviour of active yarn lengths were set by adding the required amount of NaDBS electrolyte in the electrochemical cell. In the second method, the required active lengths of the yarns were achieved by cutting the yarns, and actuation behaviour was measured. Comparing the two measurement methods, showed that active yarn length is limited by the iR drop in most cases, but that for the shorter yarn lengths using method B, electrolyte level was limiting. It also showed that there is a contribution of the wetted segment of the in-air portion to the total actuation. The resultant electroactive yarn exhibits low electrical resistance, high strain (up to 0.64 %), and good electrical stability in aqueous electrolytes. Overall, it was found that creating a full-length PPy/Ag-KDK yarns produce more strain (%) and force in comparison to PPy/KDK system in both methods. Our results also indicate that results taken from small or short samples, e.g., 1 mm, cannot be extrapolated when moving to the large size samples (e.g., long yarns) that are needed for real applications, as other effects such as iR drop or wetting/capillary effects, might give dominant contributions that reduce the performance. Further work will investigate the effect of voltage drop in actuation and the resulting efficiency of electroactive linear yarn actuators in more detail. In this work we showed actuation in a liquid electrolyte, however these CP yarn actuators can also be coated with ionic gel electrolytes. “ionogels” [43]

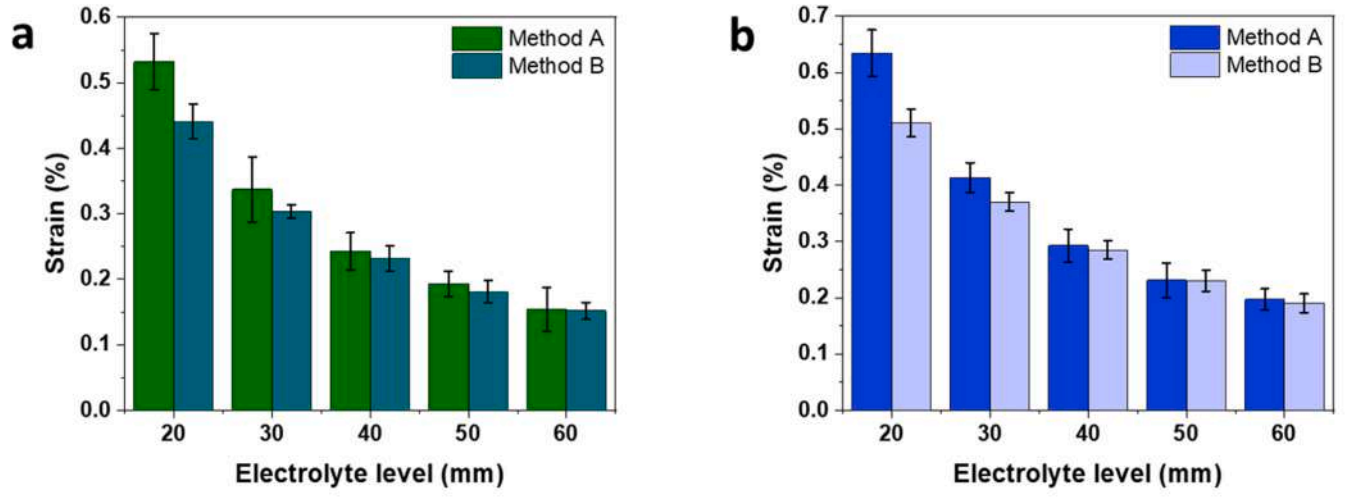

Fig. 12. Strain (%) (reduction value) comparison for (a) PPy/KDK yarns (b) PPy/Ag-KDK yarns using method A and B (From Figs. 8a and 11a).

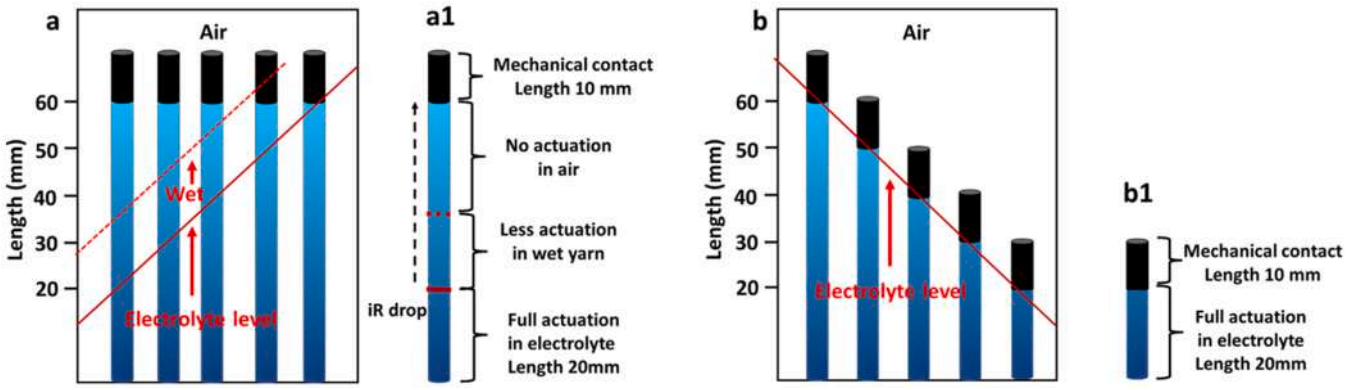

Fig. 13. Schematic diagram showing the six yarns at the various electrolyte levels and effect of voltage drop (indicated by the gradient) on the actuation for (a) method A and (b) method B.

which enables operation in air, for instance for textile muscles [44]. The yarn actuators studied here can be integrated in fabrics using knitting and weaving resulting in textile actuators or textile muscles. Such textile actuators can be seamlessly integrated in larger fabrics or garments, and thus result in fabrics or garments that provide mechanical output, the so-called 2nd generation of smart textiles [45] for potential applications such as haptic garments, soft actuators, wearable electronics, and textile exoskeletons that are lightweight, compliant and comfortable to wear.

CRediT authorship contribution statement

Sujan Dutta: Conceptualization, Methodology. **Shayan Mehraeen:** Investigation, Validation. **Nils-Krister Persson:** Investigation, Validation. **Jose G. Martinez:** Investigation, Validation. **Edwin W.H. Jager:** Conceptualization, Methodology, Supervision. All authors have read and approved the final manuscript.

Declaration of Competing Interest

There are no conflicts to declare.

Acknowledgements

The authors acknowledge the Erling-Persson Family Foundation, and European Union's Horizon 2020 research and innovation program under grant agreement no. 825232 "WEAFING" for their financial support. J.G.M. acknowledges Promobilia Foundation (F17603) for their financial support. E.W.H.J. acknowledges financial support from the Swedish Government Strategic Research Area in Materials Science on Functional Materials at Linköping University (Faculty Grant SFO Mat LiU No 2009-00971).

Appendix A. Supporting information

Supplementary data associated with this article can be found in the online version at doi:10.1016/j.snb.2022.132384.

References

[1] A. Ahmed, M.M. Hossain, B. Adak, S. Mukhopadhyay, Recent advances in 2D MXene integrated smart-textile interfaces for multifunctional applications, Chem. Mater. 32 (2020) 10296–10320.
[2] Z. Lin, J. Yang, X. Li, Y. Wu, W. Wei, J. Liu, J. Chen, J. Yang, Large-scale and washable smart textiles based on triboelectric nanogenerator arrays for self-powered sleeping monitoring, Adv. Funct. Mater. 28 (2018) 1704112–1704119.
[3] J. Zhou, M. Mulle, Y. Zhang, X. Xu, E.Q. Li, F. Han, S.T. Thoroddsen, G. Lubineau, High-ampacity conductive polymer microfibers as fast response wearable heaters and electromechanical actuators, J. Mater. Chem. C. 4 (2016) 1238–1249.
[4] L. Zhang, W. Viola, T.L. Andrew, High energy density, super-deformable, garment-integrated microsupercapacitors for powering wearable electronics, ACS Appl. Mater. Interfaces 10 (2018) 36834–36840.
[5] Q. Huang, D. Wang, Z. Zheng, Textile-based electrochemical energy storage devices, advanced energy, Materials 6 (2016) 1600783–1600813.
[6] M. Barakzehi, M. Montazer, F. Sharif, T. Norby, A. Chatzitakis, A textile-based wearable supercapacitor using reduced graphene oxide/polypyrrole composite, Electrochim. Acta 305 (2019) 187–196.
[7] V. Kaushik, J. Lee, J. Hong, S. Lee, S. Lee, J. Seo, C. Mahata, T. Lee, Textile-based electronic components for energy applications: Principles, problems, and perspective, Nanomaterials 5 (2015) 1493–1531.
[8] Y. Wu, Y. Yang, C. Li, Y. Li, W. Chen, Flexible and electroactive textile actuator enabled by PEDOT:PSS/MOF-derivative electrode ink, Front. Bioeng. Biotechnol. 8 (2020) 212.
[9] Z. Zhang, L. Cui, X. Shi, X. Tian, D. Wang, C. Gu, E. Chen, X. Cheng, Y. Xu, Y. Hu, J. Zhang, L. Zhou, H.H. Fong, P. Ma, G. Jiang, X. Sun, B. Zhang, H. Peng, Textile display for electronic and brain-interfaced communications, Adv. Mater. 30 (2018) 1800323–1800331.
[10] M. Amjadi, K.U. Kyung, I. Park, M. Sitti, Stretchable, skin-mountable, and wearable strain sensors and their potential applications: a review, Adv. Funct. Mater. 26 (2016) 1678–1698.
[11] M. Liu, X. Pu, C. Jiang, T. Liu, X. Huang, L. Chen, C. Du, J. Sun, W. Hu, Z.L. Wang, Large-area all-textile pressure sensors for monitoring human motion and physiological signals, Adv. Mater. 29 (2017) 1703700–1703709.
[12] A. Maziz, A. Concas, A. Khaldi, J. Stålhand, N.-K. Persson, E.W.H. Jager, Knitting and weaving artificial muscles, Sci. Adv. 3 (2017) 1600327–1600329.
[13] S. Seyedin, J.M. Razal, P.C. Innis, A. Jeiranikhameneh, S. Beirne, G.G. Wallace, Knitted strain sensor -textiles of highly conductive all-polymeric fibers, ACS Appl. Mater. Interfaces 7 (2015) 21150–21158.
[14] R. Gerhard, J. Su, Y. Tajitsu, S. Bauer, S. Bauer-Gogonea, Piezoelectric and Electrostrictive Polymers, 2016.
[15] F. Carpi, R. Kornbluh, P. Sommer-Larsen, G. Alici, Electroactive polymer actuators as artificial muscles: are they ready for bioinspired applications?, Bioinspiration and Biomimetics 6 (2011) 45006–45016.
[16] S. Bauer, R. Gerhard-Multhaupt, G.M. Sessler, Ferroelectrets: soft electroactive foams for transducers, Phys. Today 57 (2004), 47–45.
[17] J.G. Martinez, K. Richter, N.K. Persson, E.W.H. Jager, Investigation of electrically conducting yarns for use in textile actuators, Smart Mater. Struct. 27 (2018) 074004–074015.
[18] Q. Zhou, J. Shao, Q. Zhou, J. Chen, T. Zhou, In situ polymerization of polyaniline on cotton fabrics with phytic acid as a novel efficient dopant for flame retardancy and conductivity switching, N. J. Chem. 44 (2020) 3504–3513.
[19] G.B. Tseghai, D.A. Mengistie, B. Malengier, K.A. Fante, L. van Langenhove, PEDOT:PSS-based conductive textiles and their applications, Sens. (Switz.) 20 (2020) 1881–1898.
[20] R. Sarabia-Riquelme, R. Andrews, J.E. Anthony, M.C. Weisenberger, Highly conductive wet-spun PEDOT:PSS fibers for applications in electronic textiles, J. Mater. Chem. C. 8 (2020) 11618–11630.
[21] D. Melling, S. Wilson, E.W.H. Jager, The effect of film thickness on polypyrrole actuation assessed using novel non-contact strain measurements, Smart Mater. Struct. 22 (2013) 104021–104031.
[22] J.G. Martinez, T.F. Otero, E.W.H. Jager, Effect of the electrolyte concentration and substrate on conducting polymer actuators, Langmuir 30 (2014) 3894–3904.
[23] S. Hara, T. Zama, W. Takashima, K. Kaneto, Artificial muscles based on polypyrrole actuators with large strain and stress induced electrically, Polym. J. 36 (2004) 151–161.
[24] F. Escobar-Teran, J.G. Martinez, N.-K. Persson, W.H. Edwin, Jager, Enhancing the conductivity of the Poly(3,4-ethylenedioxythiophene)-Poly(styrenesulfonate) coating and its effect on the performance of yarn actuators, Adv. Intell. Syst. 2 (2020) 1900184.
[25] T. Bashir, M. Ali, N.K. Persson, S.K. Ramamoorthy, M. Skrifvars, Stretch sensing properties of conductive knitted structures of PEDOT-coated viscose and polyester yarns, Text. Res. J. 84 (2014) 323–334.
[26] S. Aziz, J.G. Martinez, B. Salahuddin, N.K. Persson, E.W.H. Jager, Fast and high-strain electrochemically driven yarn actuators in twisted and coiled configurations, Adv. Funct. Mater. 31 (2021), 2008959–2008959.

[27] A. Maziz, A. Khaldi, N.-K. Persson, E.W.H. Jager, Soft linear electroactive polymer actuators based on polypyrrole, in: Electroactive Polymer Actuators and Devices (EAPAD) 2015, SPIE, 2015, pp. 943016–943022.
[28] P.G.A. Madden, J.D.W. Madden, P.A. Anquetil, N.A. Vandesteeg, I.W. Hunter, The relation of conducting polymer actuator material properties to performance, IEEE J. Ocean. Eng. 29 (2004) 696–705.
[29] L. Bay, K. West, N. Vlachopoulos, S. Skaarup, Potential profile in a conducting polymer strip, in: Smart Structures and Materials 2001: Electroactive Polymer Actuators and Devices, SPIE, 2001, pp. 54–58.
[30] A. Fannir, C. Plesse, G.T.M. Nguyen, F. Vidal, Electro-interpenetration as tool for high strain trilayer conducting polymer actuator, Smart Mater. Struct. 30 (2021) 025041–025052.
[31] J. Ding, L. Liu, G.M. Spinks, D. Zhou, G.G. Wallace, J. Gillespie, High performance conducting polymer actuators utilising a tubular geometry and helical wire interconnects, Synth. Met. 138 (2003) 391–398.
[32] G.M. Spinks, T.E. Campbell, G.G. Wallace, Force generation from polypyrrole actuators, Smart Mater. Struct. 14 (2005) 406–412.
[33] A.S. Hutchison, T.W. Lewis, S.E. Moulton, G.M. Spinks), G.G. Wallace, Development of polypyrrole-based electromechanical actuators, Synth. Met. 113 (2000) 121–127.
[34] H.R. Kim, T. Ito, B.S. Kim, Y. Watanabe, I.S. Kim, Mechanical properties, morphologies, and microstructures of novel electrospun metallized nanofibers, Adv. Eng. Mater. 13 (2011) 376–382.
[35] S. Zhao, B. Guo, G. Han, Y. Tian, Metallization of electrospun polyacrylonitrile fibers by gold, Mater. Lett. 62 (2008) 3751–3753.
[36] T. Bashir, M. Skrifvars, N.K. Persson, Synthesis of high performance, conductive PEDOT-coated polyester yarns by OCVD technique, Polym. Adv. Technol. 23 (2012) 611–617.
[37] A. della Santa, D. de Rossi, A. Mazzoldi, Performance and work capacity of a polypyrrole conducting polymer linear actuator, Synth. Met. 90 (1997) 93–100.
[38] R. Khadka, N. Aydemir, A. Kesküla, T. Tamm, J. Travas-Sejdic, R. Kiefer, Enhancement of polypyrrole linear actuation with poly(ethylene oxide), Synth. Met. 232 (2017) 1–7.
[39] A. Baudler, I. Schmidt, M. Langner, A. Greiner, U. Schroder, Does it have to be carbon? Metal anodes in microbial fuel cells and related bioelectrochemical systems, Energy Environ. Sci. 8 (2015) 2048–2055.
[40] J.G. Martinez, M. Ayán-Varela, J.I. Paredes, S. Villar-Rodil, S.D. Aznar-Cervantes, T.F. Otero, Electrochemical synthesis and characterization of flavin mononucleotide-exfoliated pristine graphene/polypyrrole composites, ChemElectroChem 4 (2017) 1487–1497.
[41] E. Smela, Microfabrication of PPy microactuators and other conjugated polymer devices, J. Micromech. Microeng. 9 (1999) 1–18.
[42] L. Bay, T. Jacobsen, S. Skaarup, K. West, Mechanism of actuation in conducting polymers: osmotic expansion, J. Phys. Chem. B 105 (2001) 8492–8497.
[43] Y. Zhong, G.T.M. Nguyen, C. Plesse, F. Vidal, W.H. Edwin, Jager, Highly conductive, photolithographically patternable ionogels for flexible and stretchable electrochemical devices, ACS Appl. Mater. Interfaces 10 (2018) 21601–21611.
[44] S. Mehraeen, M. Asadi, J.G. Martinez, N.-K. Persson, E. Jager, 'Smart yarns as the building blocks of textile actuators', presented at the 9th international conference on Electromechanically Active Polymer (EAP)transducers & artificial muscles, Dresden, Germany, 4–6 June, 2019.
[45] N.K. Persson, J.G. Martinez, Y. Zhong, A. Maziz, E.W.H. Jager, Actuating textiles: next generation of smart textiles, Adv. Mater. Technol. 3 (2018) 1–12.

Sujan Dutta is a post-doctoral research fellow at the Department of Physics, Chemistry and Biology (IFM). He received an M.Sc. degree in chemistry from the National Institute of Technology, Rourkela, India in 2010 and a Ph. D. degree in Chemistry from the Indian Institute of Technology, Kharagpur, India in 2016. Prior to joining LiU, he worked as a Postdoctoral Research Fellow at the Institute of Chemistry, Hebrew University of Jerusalem, Israel. His current research includes textile-based actuators and 3D printed shape memory polymer (SMPs) by a stereolithography process.

Shayan Mehraeen is postdoc researcher at the department of physics, chemistry, and biology (IFM), Linköping University (Sweden). He obtained his Ph.D. degree in materials science and engineering from Sabanci University (Turkey) in 2018 on development of soft polymeric actuators based on conductive polymers. His research interests include conductive polymers, electrochemistry, and textile actuators for wearables.

Nils-Krister Persson, ass professor, docent, is head of Smart Textiles Technology Lab and Persson Research Group Polymer E- textiles at Swedish School of Textiles, University of Borås, Borås, Sweden. He has a long history within the smart textile community in both research and innovation together with industry and other organizations. Before entering into textiles, he worked long with organic electronics. Research interests includes conductive textile fibres, fibretronic, textile actuation, medical application of smart textiles, water purification, textile tactile communication and sensetech.

Jose G. Martinez is assistant professor in the division of Sensors and Actuators Systems at the Department of Physics, Chemistry and Biology (IFM), Linköping University. He received his PhD in 2015 from the Universidad Politécnica de Cartagena (Spain). The dissertation was awarded with the 'best Ph.D. dissertation of the university' and the 'Antonio Aldaz' (from the Electrochemistry group of the Spanish Royal Society of Chemistry) awards. His research is focused on the study of conducting polymers, from their basic principles to their applications, mainly focused on actuators.

Edwin Jager is Associated Professor and head of the division of Sensor and Actuator Systems. He received his M.Sc.Eng. degree (ir) in Applied Physics at University of Twente, The Netherlands in 1996, specializing in transduction science. In 2001, he received his PhD in Applied Physics at Linköping University, Sweden.His research interests include electroactive polymers, conducting polymer (micro-) actuators, bionics, bioelectronic medicine, electroactive surfaces and scaffolds, textile actuators, and polymer (micro-) actuators for cellular mechano-biology (mechano-transduction), medical devices and soft (micro-) robotics.